

Revisit of generalized Kerker's conditions using composite metamaterials

Rfaqat Ali^{1,*}

¹*Instituto de Física, Universidade Federal do Rio de Janeiro,
Caixa Postal 68528, Rio de Janeiro, RJ, 21941-972, Brasil*

Achieving zero backward scattering (ZBS) and zero forward scattering (ZFS), i.e., the so-called the first and second Kerker's conditions respectively, by sphere spherical particles is considered to be impossible due to the unavailability of naturally occurring magnetic materials in the visible frequency range. We report theoretical modeling to design composite metamaterials that present large optical magnetic permeability in the visible frequency range by employing Mie scattering theory and extended Maxwell Garnett theory. We numerically show that a careful selection of constituents of a composite metamaterial one can obtain metamaterials with sufficiently large artificial permeability that eventually provides the Kerker's criterion to achieve the Kerker's conditions. By taking realistic material parameters we demonstrate that the metamaterials exhibiting ZBS and ZFS have a small imaginary part of the refractive index than metallic structures that pave a path to design high-performance nanophotonic devices.

I. INTRODUCTION

Optimal control on directional scattering by spherical particles in the visible frequency domain is an ultimate goal for researchers to optimize the efficiency of optical devices [1–7]. For referential examples, the desire to achieve zero backscattering plays a crucial role in optical manipulation of spherical particles [8–10] and light management structures used in photovoltaic devices [11, 12]. The Mie scattering theory provides an exact solution to the problem of light scattering by spheres [13] and the seminal work on directional scattering was presented by Kerker et al. in 1983 [14]. They revealed proper combinations of relative permittivity and relative permeability of an unconventional magneto-dielectric sphere to achieve ZBS and ZFS that are commonly known as the first and second Kerker's conditions, respectively. Fulfillment of the first Kerker's condition requires a material with identical relative permittivity ϵ and relative permeability μ (i.e. $\epsilon = \mu$), while the second Kerker's condition needs material with $\epsilon = \frac{4-\mu}{\mu+2}$. Observation of these conditions for the visible light is considered to be impossible due to the unavailability of such materials that possess large relative magnetic permeability in the frequency range, thus, Kerker's method can not be applied in optical frequencies.

However, in spite of these limitations ZBS and ZFS are successfully experimentally demonstrated by a dipolar sphere of large permittivity [15, 16]. In this case, the incident field equally excites the electric and magnetic dipoles that produce anisotropic scattering pattern. Since the anisotropic distribution of the scattered field is governed by the interference between the electric and magnetic dipoles. For instance, the in-phase and out of phase oscillations of the electric and magnetic dipoles can provide an opportunity to observe ZBS and ZFS, respec-

tively [17–20]. Although these proposals are limited to the sphere of small radius (r) as compared to the incident wavelength (λ), such that $r \ll \lambda$.

Nowadays, the anomalous but very fascinating scattering behavior is observed by artificially designed so-called metamaterials with unconventional optical constants [21, 22]. They have the ability to present unique scattering properties like optical cloaking [23], negative optical reflection [24] and efficient control on scattering directionality [10] with valuable interest in the fields of nanoantenna, nano waveguides and optical manipulations [10, 25–27]. The recent advancement in the field of metamaterials allows to achieve the invisibility of an object through scattering cancellation by manipulating the optical permittivity and permeability of the materials [23, 28]. Although, it is challenging to find appropriate materials to design the metamaterial that presents a strong artificial magnetism in the visible range. Recently, the ZBS has been shown by a sphere made of composite metamaterial [10] by tuning the permittivity of the sphere in such a way that electric and magnetic multipoles interfere destructively in the backward direction, thus ZBS is achieved. This proposal is neither robust against the radius nor accommodates the permeability of the sphere, while the Kerker's method is applicable for all radii.

Motivated by the recent advancement in the field of metamaterials, in this article, we put forward a composite material platform to design composite metamaterials that exhibit strong artificial magnetic response in the optical frequencies range. Furthermore, we engineer the optical constants of the composite metamaterials to meet the Kerker's criterion to achieve the ZBS and ZFS. In order to implement this proposal, we consider a composite metamaterial made of a dielectric host medium containing dipolar spherical inclusions of large optical permittivity [23, 29, 30]. Furthermore, we apply extended Maxwell-Garnett theory to calculate the effective optical constants of homogenized composite metamaterials in the optical frequency range by assuming that the sizes of the inclusions are sufficient to overcome the nonlocal

*r.ali@if.ufrj.br

effects [31, 32]. In addition, the Mie scattering theory is used to calculate the relevant directional scattering cross sections of the composite metamaterials.

The rest of the article is organized as follows. Section II is a methodological part, where the Mie scattering theory and extended Maxwell-Garnett (EMG) theory are briefly discussed. The main findings of the work are presented in sections III, where the Kerker's conditions for composite metamaterials are analyzed. Finally, we summarize our findings in section IV.

II. METHODOLOGY

A. Mie Theory

Consider a plane wave with vacuum wavelength λ_0 scattering by a spherical particle of radius r , refractive index $n = \sqrt{\epsilon\mu}$ embedded in a non-absorbing host medium with refractive index $n_1 = \sqrt{\epsilon_1\mu_1}$, where $\epsilon(\epsilon_1)$ and $\mu(\mu_1)$ are the relative permittivity and relative permeability of the sphere (host medium). The scattering and absorption of incident light by the sphere is described by the Mie scattering theory in terms of normalized scattering efficiency Q_{sca} , absorption efficiency Q_{abs} , extinction efficiency Q_{ext} and mathematically defined as [13, 17, 18, 33]

$$Q_{sca} = \frac{2}{x^2} \sum_{\ell=1}^{\infty} (2\ell+1)(|a_{\ell}|^2 + |b_{\ell}|^2), \quad (1)$$

$$Q_{abs} = \frac{2}{x^2} \sum_{\ell=1}^{\infty} (2\ell+1)(\text{Re}[a_{\ell}] - |a_{\ell}|^2 + \text{Re}[b_{\ell}] - |b_{\ell}|^2), \quad (2)$$

$$Q_{ext} = Q_{abs} + Q_{sca}, \quad (3)$$

where a_{ℓ} and b_{ℓ} are the Mie scattering coefficients corresponding to the transverse magnetic and transverse electric modes, respectively. The index ℓ is used to denote ℓ^{th} order spherical harmonic channel and $x = kr$ is size parameter with $k = 2\pi/\lambda$. The Mie scattering coefficients can be derived by employing the boundary conditions on the surface of the scatterer and written as [13]

$$a_{\ell} = \frac{m\psi_{\ell}(mx)\psi'_{\ell}(x) - \mu\psi_{\ell}(x)\psi'_{\ell}(mx)}{m\psi_{\ell}(mx)\xi'_{\ell}(x) - \mu\xi_{\ell}(x)\psi'_{\ell}(mx)}, \quad (4)$$

$$b_{\ell} = \frac{\mu\psi_{\ell}(mx)\psi'_{\ell}(x) - m\psi_{\ell}(x)\psi'_{\ell}(mx)}{\mu\psi_{\ell}(mx)\xi'_{\ell}(x) - m\xi_{\ell}(x)\psi'_{\ell}(mx)}, \quad (5)$$

where, ψ_{ℓ} , ξ_{ℓ} are Riccati-Bessel functions [34], $m = n/n_1$ is the relative refractive index. In order to study the

directional scattering pattern, the expressions for differential scattering efficiencies in forward ($\theta = 0$) and backward ($\theta = \pi$) directions are given as [13]

$$Q_b|_{\theta=\pi} = \frac{1}{x^2} \left| \sum_{\ell=1}^{\infty} (2\ell+1)(-1)^{\ell}(a_{\ell} - b_{\ell}) \right|^2, \quad (6)$$

$$Q_f|_{\theta=0} = \frac{1}{x^2} \left| \sum_{\ell=1}^{\infty} (2\ell+1)(a_{\ell} + b_{\ell}) \right|^2. \quad (7)$$

It can be seen in Eq. (6), the first Kerker's condition (i. e. $Q_b = 0$) can be achieved by providing $a_{\ell} = b_{\ell}$ and this can occur for identical permittivity and permeability of the sphere (see Eqs. 4-5). On the other hand, the second Kerker's condition can be satisfied by achieving $Q_f \simeq 0$, provided that $a_1 \simeq -b_1$, this occurs when the condition $\epsilon = \frac{4-\mu}{2\mu+1}$ is satisfied in the quasi-static limit.

It is worthwhile to mention that the optical theorem imposes a severe condition to achieve ZFS. This theorem of optics relates the extinction cross section σ^{ext} to the forward scattering amplitude $s_{\theta}(0,0)$ and can be expressed as $\sigma^{ext} = \frac{\lambda_0^2}{\pi} \text{Im}[s_{\theta}(0,0)]$ [35, 36]. In practice, $Q_f = 0$ (at 2nd Kerker's condition) appears by achieving $a_1 = -b_1$ without necessarily making both of them zero [14], which not only vanishes the forward scattering but also nullify the total extinction cross section (one may refer to Eq. (3) in quasi-static approximation). Subsequently, the non zero a_1 and b_1 are implying that the overall scattering in all other directions may still be significantly different from zero, which seems to be a contradiction to the fact that extinction cross section vanishes. However, the usual approximation for the dipole coefficients fail to satisfy energy conservation requirements [35]. A more accurate approximation for those coefficients, taking into account radiative corrections, shows that the forward scattering is not exactly zero, relaxing the contradiction. Therefore, one cannot completely suppress the forward scattering, it may be possible to achieve near zero forward scattering (NZFS) at second Kerker's condition. In order to demonstrate these conditions, we use the effective medium theory that will provide an environment to satisfy the Kerker's conditions.

B. Extended Maxwell Garnett Theory

When electromagnetic field propagates through a heterogeneous medium comprises of non-absorbing host medium of permittivity ϵ_h and small spherical inclusions of permittivity ϵ_i , radius b , such that $b \ll \lambda$. There is a variety of effective medium theories for homogenization of the heterogeneous medium [37, 38]. The collective optical response of such a homogenized medium can be discussed by defining the effective optical constants provided by one of the effective medium theory. Due to the

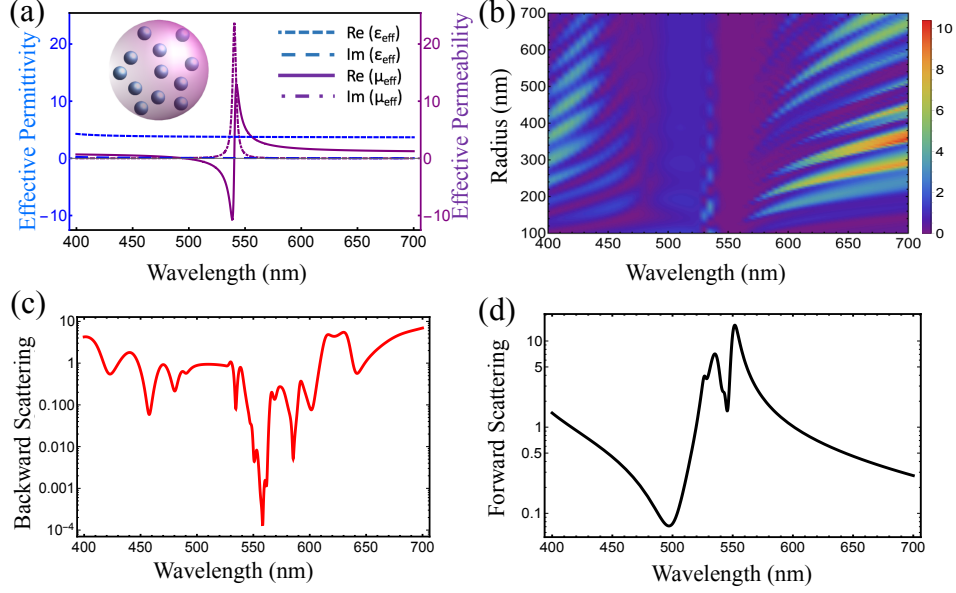


FIG. 1: (a) The real and imaginary parts of the effective permittivity (blue) and effective permeability (purple) of the composite metamaterial made of SiO_2 as a host medium and spherical inclusions of permittivity $\epsilon_i = 169$ [23], where inset shows the geometry of the composite sphere. (b) The backward scattering efficiency by the composite sphere as a function of incident wavelength and radius is plotted. (c) The backward scattering efficiency by composite sphere of radius 500 nm and (d) forward scattering efficiency by composite sphere of radius 70 nm are displayed as function of incident wavelength. Throughout the figure, the radius of the spherical inclusions and volume filling fraction are fixed at $b = 20$ nm and $f = 0.2$ respectively.

best performance we use extended Maxwell-Garnett theory [23, 39–43], which provides the effective permittivity and permeability as functions of volume filling fraction f , size of the inclusions, permeability and permittivity of the host medium as $n_{\text{eff}} = \sqrt{\epsilon_{\text{eff}} \mu_{\text{eff}}}$, where

$$\epsilon_{\text{eff}} = \epsilon_h \frac{y^3 + 3if a_1}{y^3 - \frac{3}{2}if a_1}, \quad (8)$$

$$\mu_{\text{eff}} = \mu_h \frac{y^3 + 3if b_1}{y^3 - \frac{3}{2}if b_1}. \quad (9)$$

Here $y = \sqrt{\epsilon_h} \omega b / c$, is the size parameter inside the host medium, ω is the frequency, c is the speed of light, a_1 and b_1 are dipolar Mie coefficients of the inclusions. The size parameter must be $y \ll 1$ [43], otherwise higher order multipoles will contribute to effective permittivity and permeability and spoil the validity of EMG theory.

III. RESULTS AND DISCUSSIONS

We begin our numerical analysis by considering a composite material made of SiO_2 as host medium with relative permittivity $\epsilon_h = 2.1$ [44] and dielectric spherical inclusions of radius 20 nm, bulk relative permittivity $\epsilon_i = 169$ [23, 29] and volume filling fraction f . The effective optical constants of the composite material are

calculated by EMG theory (Sec. II B). Since the inclusions have a large refractive index so that the incident field can generate displacement currents inside the inclusions and produces tiny magnetic dipoles. The collective effect of these spherical magnetic dipoles generates a remarkable magnetic response in the composite metamaterials. The effective optical response of the composite metamaterials is measured in terms of effective permittivity and effective permeability by using the Eqs. (8-9) that have external degrees of freedom, like volume filling fraction, permittivities and size of inclusions. One can perform fine tuning of these parameters to tailor the resonance at a chosen wavelength for operation. In Fig. 1(a), the real and imaginary parts of the effective permittivity (blue) and permeability (purple) of the composite metamaterial are displayed as a function of incident wavelength. It is clearly seen that the composite metamaterial shows remarkable magnetic response with a spectral region that indeed lies in our domain of interest. For instance, the composite metamaterial shows an identical effective permeability and permittivity at the wavelength of 560 nm with relatively small imaginary parts. According to Kerker's method, this is an ideal scenario to satisfy the first Kerker's condition for all sized spherical particles. Fig. 1(b) shows a color map of backward scattering efficiency by the composite sphere as a function of the incident wavelength and radius of the sphere. It is clearly seen that at $\lambda = 560$ nm the backward scattering is completely suppressed which occurs

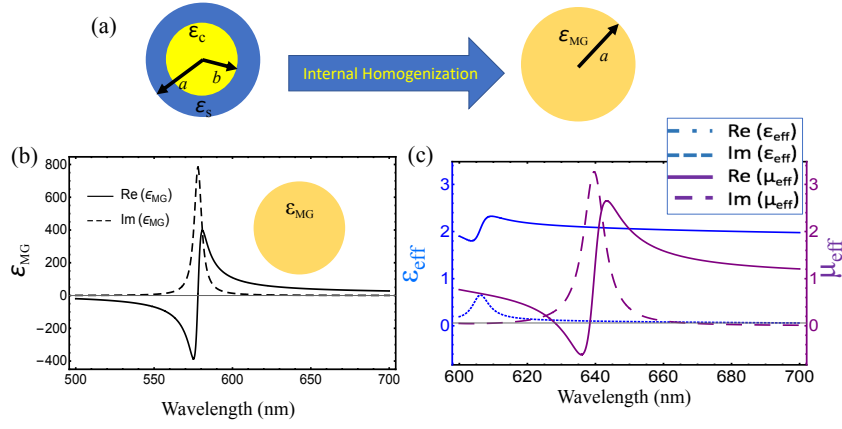


FIG. 2: (a) The schematic diagram of internal homogenization, (b) the real and imaginary parts of effective permittivity of the effective sphere. (c) The real and imaginary parts of effective permittivity and permeability of an arbitrarily arranged effective spheres in a homogeneous medium with $\epsilon_h = \mu_h = 1$ for filling fraction $f = 0.25$ as a function of incident wavelength.

due to the in-phase oscillations of the electric and magnetic multipoles with same amplitudes such that $a_\ell = b_\ell$, provided by identical ϵ_{eff} and μ_{eff} as shown in Fig. 1(a). Therefore, the overall backward scattering efficiency defined in Eq. (6) is reduced to zero regardless of the sizes of the sphere. The drastic reduction of backward scattering by the composite sphere of radius 500 nm is shown in Fig. 1(c) by calculating the backward scattering efficiency versus wavelength. It is clearly shown that the dramatic reduction appears at $\lambda = 560$ nm and backward scattering amplitude reduces to zero, thus satisfying the first Kerker's condition.

In contrast, the second Kerker's condition requires the condition $\epsilon_{\text{eff}} = \frac{4 - \mu_{\text{eff}}}{\mu_{\text{eff}} + 2}$, which surprising also occurs at a wavelength of 500 nm. In Fig. 1(d), we calculate the forward scattering efficiency by a composite sphere of radius 70 nm as a function of the incident wavelength. The drastic reduction of forward scattering appears at $\lambda = 500$ nm and satisfying the second Kerker's condition. It is worthwhile to mention that the second Kerker's condition can be achieved by providing $a_\ell = -b_\ell$, which only implies to the dipolar particles (i.e. for $\ell = 1$). Otherwise, this effect might be spoiled for a large sphere due to higher-order multipole contributions to the forward scattering efficiency. Thus, provides nearly zero forward scattering $Q_f \simeq 0$ at $\lambda = 500$ nm for a *dipolar sphere* (of radius 70 nm).

Now we extend our proposal to design metamaterials by using naturally occurring materials that will present a significant magnetic response to satisfy the Kerker's conditions. The immediate question that arises, is there any material that possesses large permittivity in the visible region? The answer is yes, for instance, a carefully designed core-shell system shows a very high permittivity due to plasmonic resonances with strong spectral dependence and in the quasi-static approximation these core-shell nanoparticles can be used as inclusions into a host medium. For simplicity, we begin with an in-

ternal homogenization approach introduced by Chettiar and Enghetta [30] that provides effective permittivity of core-shell nanoparticle by homogenizing it to an effective sphere of the same dimension. Through this approach, the effective permittivity of a core-shell nanoparticle is calculated by equating the polarizabilities of the core-shell to a homogenized sphere of the same dimension and finally, the expression turns out as

$$\epsilon_{\text{MG}} = \epsilon_s \frac{a^3(\epsilon_c + 2\epsilon_s) + 2b^3(\epsilon_c - \epsilon_s)}{a^3(\epsilon_c + 2\epsilon_s) - b^3(\epsilon_c - \epsilon_s)}. \quad (10)$$

In order to implement this proposal, we consider metallic nanosphere as a core of radius b embedded in dielectric spherical shell of radius a , forming a core-shell nanoparticle [45–48]. Assuming that the core is silver (Ag) and we may use Drude formula to define its permittivity, $\epsilon_c = \epsilon_\infty - \frac{\omega_p^2}{\omega(\omega + i\Gamma)}$, with $\omega_p = 9.2 \text{ eV}$, $\Gamma = 0.0212 \text{ eV}$, $\epsilon_\infty = 5.0$, where $1 \text{ eV} = 241.8 \text{ THz}$ [49] and ω is the angular frequency of incident light. Furthermore, the core-shell is homogenized to an effective sphere of radius a with permittivity ϵ_{MG} provided by Eq. (10) and displayed in Fig. 2(b) at fixed radii ratio at $\frac{b}{a} = 0.84$. It has been verified that in the quasi-static limit, the effective sphere has a good agreement to exact Mie solution of a core-shell nanoparticles of the same dimension [50] and indeed it can be used as inclusion into a host medium to fabricate the structures of desired optical and physical properties [30, 50–52].

Let us design a bulk composite medium comprises of randomly arranged effective (homogenized) nanospheres with permittivity ϵ_{MG} and radius a embedded in a host medium with volume filling fraction f . In Fig. 2(c) we calculate the effective permittivity (blue) and permeability (purple) of newly designed composite metamaterial by means of EMG theory at fixed $f = 0.25$ as a function of λ . In this configuration, we consider radii of the effective nanosphere about 14 times less than the incident

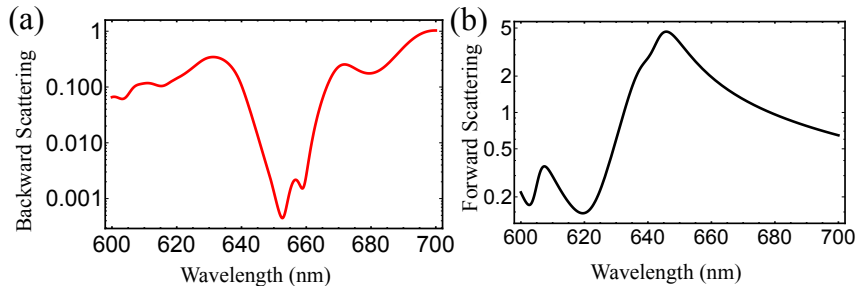


FIG. 3: (a) Backward scattering efficiency by a sphere made of composite metamaterial (of permittivity given in Fig. 2c) of radius 800 nm as a function of incident wavelength. (b) Forward scattering efficiency by a composite sphere of radius 120 nm, where the volume filling fraction is fixed at $f = 0.25$.

wavelength which is a safe zone for the validation of the effective medium theory [43].

It can be seen in Fig. 2(c) that the composite metamaterial not only presents large effective permeability but also provides identical permittivity and permeability with weak imaginary parts at a wavelength of 650 nm. Therefore, according to Kerker's criterion, it must present zero backward scattering at this wavelength. We now calculate the directional scattering by the composite sphere of radius r with permittivity given in Fig. 2(c). The backward scattering efficiency and forward scattering efficiency as a function of incident wavelength are displayed in Fig. 3(a) and 3(b), respectively. It is clearly seen that the backward scattering efficiency is drastically reduced to zero at $\lambda = 650$ nm which is due to the fact that equal electric and magnetic response. On the other hand, the NZFS appears at a wavelength of 620 nm due to out of phase oscillations of electric and magnetic dipoles, thus satisfying the second Kerker's condition.

IV. CONCLUSIONS

In this paper, we have theoretically modeled composite metamaterials using Mie scattering theory and effective medium theory. Our numerical results have shown that the composite metamaterials present strong artificial magnetic permeability in the optical frequency domain that appears due to the displacement currents inside the

inclusions. Our findings show that a fine tuning of the parameters appear in the EMG theory, one can create a spectral region with identical permittivity and permeability not only for bulk homogeneous composite spherical sphere but also for a regularly arranged nanospherical particles. *Altogether, this proposal not only paves a path to design new possible structures with artificial magnetic response but also allows to achieve Kerker's conditions for low refractive index materials in the visible frequency range.* These structures with unique optical properties have very low $\text{Im}(m_{\text{eff}})$ (i. e. low absorption) than metallic structure that makes our proposal a good candidate to design high-performance optical antennas, metamaterials and other novel nanophotonic devices.

V. ACKNOWLEDGMENT

We thank F. Pinheiro, F. Rosa, PAM Neto and S. Iqbal for inspiring discussions. This work has been supported by the Brazilian agencies National Council for Scientific and Technological Development (CNPq), Coordination for the Improvement of Higher Education Personnel (CAPES).

VI. REFERENCES

-
- [1] A. G. Curto, et al. *Unidirectional emission of a quantum dot coupled to a nanoantenna*, Science **329**, 930 (2010).
 - [2] D. Gao, W. Ding, M. Nieto-Vesperinas, et al. *Optical manipulation from the microscale to the nanoscale: fundamentals, advances and prospects*, Light Sci. & App. **6**, e17039 (2017).
 - [3] A. V. Kabashin, P. Evans, S. Pastkovsky, et al. *Plasmonic nanorod metamaterials for biosensing*, Nat. Mater. **8**, 867 (2009).
 - [4] A. Ahmed and R. Gordon, *Single molecule directivity enhanced raman scattering using nanoantennas*, Nano Lett. **12**, 2625 (2012).
 - [5] W. Liu, A. E. Miroshnichenko, D. N. Neshev and Y. S. Kivshar, *Broadband unidirectional scattering by magneto-electric coreshell nanoparticles*, ACS Nano **6**, 5489 (2012).
 - [6] Y. F. Tao, Z. Y. Guo, Y. X. Sun, et al. *Sliver spherical nanoshells coated gain-assisted ellipsoidal silica core for*

- low-threshold surface plasmon amplification, *Opt. Commun.* **355**, 580 (2015).
- [7] M. Kuo, Y. Kim, M. Hsieh and S. Lin, *Efficient and directed nano-LED emission by a complete elimination of transverse-electric guided modes*, *Nano Lett.* **11**, 476 (2011).
 - [8] J. Chen, J. Ng, Z. Lin and C. T. Chan, *Optical pulling force*, *Nat. Photon.* **5**, 531 (2011).
 - [9] N. O. Länk, P. Johansson and Mikael Käll, *Directional scattering and multipolar contributions to optical forces on silicon nanoparticles in focused laser beams*, *Opt. Exp.* **26**, 29074 (2018).
 - [10] R. Ali, F. A. Pinheiro, F. S. S. Rosa, R. S. Dutra and P. A. Maia Neto, *Optimizing optical tweezing with directional scattering in composite microspheres*, *Phys. Rev. A* **98**, 053804 (2018).
 - [11] V. E. Ferry, J. N. Munday and H. A. Atwater, *Design considerations for plasmonic photovoltaics*, *Adv. Mater.* **22**, 4794 (2010).
 - [12] Y. A. Akimov, W. Koh, S. Sian and S. Ren, S. Nanoparticle-enhanced thin film solar cells: metallic or dielectric nanoparticles?, *Appl. Phys. Lett.* **96**, 073111 (2010).
 - [13] C. F. Bohren and D. R. Huffman, *Absorption and scattering of light by small particles* (Wiley, 1983).
 - [14] M. Kerker, D. Wang and C. J. Giles, *Electromagnetic scattering by magnetic spheres*, *Opt. Soc. A* **73**, 765 (1983).
 - [15] Y. H. Fu, A. I. Kuznetsov, A. E. Miroshnichenko, Ye F. Yu and B. Lukyanchuk, *Directional visible light scattering by silicon nanoparticles*, *Nat. Commun.* **4**, 1527 (2013).
 - [16] S. Person, M. Jain, Z. Lapin, J. J. Sáenz, G. Wicks and L. Novotny, *Demonstration of zero optical backscattering from single nanoparticles*, *Nano Lett.* **13**, 1806 (2013).
 - [17] R. Gomez-Medina et al. *Electric and magnetic dipolar response of Germanium spheres: Interference effects, scattering anisotropy and optical forces*, *Journal of nanophotonics* **5**, 053512 (2011).
 - [18] Y. Li, Wan et al. *Broadband zero-backward and near-zero-forward scattering by metallo-dielectric core-shell nanoparticles*, *Sci. Rep.* **5**, 12491 (2015).
 - [19] Y. Zhang, M. N. Vesperinas and J. J. Saenz, *Dielectric spheres with maximum forward scattering and zero backscattering: a search for their material composition*, *J. Opt.* **17**, 105612 (2015).
 - [20] J. Geffrin, B. García-Cámara, R. Gómez-Medina et al. *Magnetic and electric coherence in forward- and back-scattered electromagnetic waves by a single dielectric sub-wavelength sphere*, *Nat. Commun.* **3**, 1171 (2012).
 - [21] N. Engheta and R. W. Ziolkowski, *Metamaterials: physics and engineering explorations*, (John Wiley and Sons 2006).
 - [22] R. Maas, J. Parsons, N. Engheta and A. Polman *Experimental realization of an epsilon-near-zero metamaterial at visible wavelengths*, *Nat. Photonics*, **7**, 907 (2013).
 - [23] M. Farhat, S. Mühlig, C. Rockstuhl and F. Lederer, *Scattering cancellation of the magnetic dipole field from macroscopic spheres*, *Opt. Exp.* **20**, 13896 (2012).
 - [24] B. Knoll and F. Keilmann, *Enhanced dielectric contrast in scattering-type scanning near-field optical microscopy*, *Opt. Commun.* **182**, 321 (2000).
 - [25] F. Moreno, P. Albella and M. N. Vesperinas, *Analysis of the spectral behavior of localized plasmon resonances in the near-and far-field regimes*, *Langmuir* **29**, 6715 (2013).
 - [26] R. Alaei, R. Filter, D. Lehr, F. Lederer and C. Rockstuhl, *A generalized Kerker condition for highly directive nanoantennas*, *Opt. Lett.* **40**, 2645 (2015).
 - [27] N. Wang, X. Li, J. Chen et al. *Gradient and scattering forces of anti-reflection-coated spheres in an aplanatic beam*, *Sci. Rep.* **8**, 17423 (2018).
 - [28] C. Soukoulis and M. Wegener, *Past achievements and future challenges in the development of three-dimensional photonic metamaterials*, *Nat. Photon.* **5**, 523 (2011).
 - [29] D. V. Goia, et al. *Precipitation and recrystallization of uniform CuCl particles formed by aggregation of nano-sized precursors*, *Colloid Polymer Sci.* **281**, 754 (2003).
 - [30] U. K. Chettiar and N. Engheta, *Internal homogenization: Effective permittivity of a coated sphere*, *Opt. Exp.* **20**, 22976 (2012).
 - [31] R. Ruppin, *Optical properties of a plasma sphere*, *Phys. Rev. Lett.* **31**, 1434 (1973).
 - [32] C. R. Gubbin and S. De Liberato, *Optical nonlocality in polar dielectrics*, *Phys. Rev. X* **10**, 021027 (2020).
 - [33] H. C. van de Hulst, *Light scattering by small particles*, New York (John Wiley and Sons) (1957).
 - [34] *NIST digital library of mathematical functions*, <http://dlmf.nist.gov/25.12>, release 1.0.16 of 2017-09-18, edited by F. W. J. Olver, A. B. Olde Daalhuis, D. W. Lozier, B.I. Schneider, R. F. Boisvert, C. W. Clark, B. R. Miller and B. V. Saunders.
 - [35] A. Alú and N. Engheta, *How does zero forward-scattering in magnetodielectric nanoparticles comply with the optical theorem ?*, *J. Nanophoton.* **4**, 041590 (2010).
 - [36] J. Yi Lee, A. E. Miroshnichenko and R. Lee, *Simultaneously nearly zero forward and nearly zero backward scattering objects*, *Opt. Exp.* **26**, 30393 (2018).
 - [37] T. C. Choy, *Effective medium theory: principles and applications* (Oxford University Press, Oxford, 2015).
 - [38] W. T. Doyle, *Optical properties of a suspension of metal spheres*, *Phys. Rev. B* **39**, 9852 (1989).
 - [39] S. Mühlig, A. Cunningham, J. Dintinger, M. Farhat, S. B. Hasan, T. Scharf, T. Burgi, F. Lederer and C. Rockstuhl, *A self-assembled three-dimensional cloak in the visible*, *Sci. Rep.* **3**, 2328 (2013).
 - [40] R. Ali, F. A. Pinheiro, R. S. Dutra, F. S. S. Rosa and P. A. M. Neto, *Enantioselective manipulation of single chiral nanoparticles using optical tweezers*, *Nanoscale* **12**, 5031 (2020).
 - [41] S. Mühlig, A. Cunningham, J. Dintinger, T. Scharf, T. Bürgi, F. Lederer and C. Rockstuhl, *Self-assembled plasmonic metamaterials*, *Nanophotonics* **2**, 0036 (2012).
 - [42] P. Mallet, C. A. Guerin and A. Sentenac, *Maxwell-Garnett mixing rule in the presence of multiple scattering: derivation and accuracy*, *Phys. Rev. B* **72**, 014205 (2005).
 - [43] R. Ruppin, *Evaluation of extended Maxwell-Garnett theories*, *Opt. Commun.* **182**, 273 (2000).
 - [44] I. H. Malitson, *Interspecimen comparison of the refractive index of fused silica*, *J. Opt. Soc. Am.* **55**, 1205 (1965).
 - [45] N. Hagurua, W. Widiyastuti, F. Iskandar and K. Okuyama, *Characterization of silica-coated silver nanoparticles prepared by a reverse micelle and hydrolysis-âcondensation process*, *Chemical Engineering Journal* **156**, 200 (2010).
 - [46] S. J. Oldenburg, R. D. Averitt, S. L. Westcott and N. J. Halas, *Nanoengineering of optical resonances*, *Chem.*

- Phys. Lett. **288**, 243 (1998).
- [47] R. G. Chaudhuri and S. Paria, *Core/shell nanoparticles: classes, properties, synthesis mechanisms, characterization, and applications*, Chem. Rev. **112**, 2373 (2012).
 - [48] C. Hanske, M. N. Sanz-Ortiz and L. M. Liz-Marzán, *Silica-coated plasmonic metal nanoparticles in action*, Adv. Mater. **30**, 1707003 (2018).
 - [49] P. B. Johnson and R. W. Christy, *Optical constants of the noble metals*, Phys. Rev. B **6**, 4370 (1972).
 - [50] Y. Gutiérrez, D. Ortiz, R. A. de la Osa, J. M. Saiz, F. González and F. Moreno, *Electromagnetic effective medium modelling of composites with metal-semiconductor core-shell type inclusions*, Catalysts **9**, 626 (2019).
 - [51] Aitzol G. Etxarri, et al. *Strong magnetic response of submicron silicon particles in the infrared*, Opt. Exp. **19**, 4815 (2011).
 - [52] R. Dezert, P. Richetti and A. Baron, *Isotropic Huygens dipoles and multipoles with colloidal particles*, Phys. Rev. B **96**, 180201(R) (2017).